

1 **Quantifying the Value of Learning for Flexible Water Infrastructure Planning**

2 **J. B. Skerker<sup>1</sup>, M. Zaniolo<sup>1</sup>, K. Willebrand<sup>1</sup>, M. Lickley<sup>2,3</sup>, and S. M. Fletcher<sup>1,4\*</sup>**

3 <sup>1</sup>Civil and Environmental Engineering, Stanford University

4 <sup>2</sup>Science, Technology and International Affairs, Edmund A. Walsh School of Foreign Service,  
5 Georgetown University

6 <sup>3</sup>Earth Commons, Georgetown University

7 <sup>4</sup>Woods Institute for the Environment, Stanford University

8 \* corresponding author

9 Corresponding author: Sarah Fletcher ([sfletcher@stanford.edu](mailto:sfletcher@stanford.edu))

10 **Key Points:**

- 11 • We present a framework to assess how the rate of learning about climate uncertainty  
12 affects the value of flexible water infrastructure
- 13 • Exploratory Bayesian modeling generates climate learning scenarios with high and low  
14 potential to reduce future precipitation uncertainty
- 15 • In a case study in Mombasa, Kenya, flexible water infrastructure is valuable in high-  
16 learning scenarios and wet precipitation conditions

17 **Abstract**

18 Uncertainty in future climate change challenges water infrastructure development decisions.  
 19 Flexible infrastructure development, in which infrastructure is proactively designed to be  
 20 changed in the future, can reduce the risk of overbuilding unnecessary infrastructure while  
 21 maintaining reliable water supply. Flexible strategies assume that water planners will learn over  
 22 time, updating future climate projections and using that new information to change plans.  
 23 Previous work has developed methods to incorporate learning using climate observations into  
 24 flexible planning but has not quantified the impact of different amounts of learning on the  
 25 effectiveness of flexible planning. In this work, we develop a framework to assess how  
 26 differences in the amount of learning about climate uncertainty affect the value of flexible water  
 27 infrastructure planning. In the first part of our framework, we design climate scenarios with  
 28 different amounts of learning using an exploratory Bayesian modeling approach. Then, we  
 29 quantify the impacts of learning on flexibility using simulated costs and infrastructure decisions.  
 30 We demonstrate this framework on a stylized case study of the Mwache Dam near Mombasa,  
 31 Kenya. Flexible planning is more effective in avoiding over- or underbuilding under high-  
 32 learning scenarios, especially in avoiding overbuilding in wet climates. This framework provides  
 33 insight on the climate conditions and learning scenarios that make flexible infrastructure most  
 34 valuable.

35 **1 Introduction**

36 Climate change uncertainty challenges water supply planning (Gleick, 1989, 2000).  
 37 Infrastructure systems, which are designed to last for many decades, must perform well under  
 38 highly uncertain conditions (Cosgrove & Loucks, 2015; IPCC, 2022). Traditional water supply  
 39 planning approaches usually oversize water infrastructure using a safety factor to account for  
 40 uncertainty and reduce the chance of system failure (Stakhiv, 2011). However, overbuilding adds  
 41 costs and environmental impacts, which are especially detrimental in more resource-scarce  
 42 regions. One strategy to plan under uncertainty is flexible planning. Flexible, or adaptive,  
 43 planning approaches can help mitigate infrastructure over- or underbuilding by changing the  
 44 design or operations of infrastructure to respond to evolving conditions over time (Bertoni et al.,  
 45 2021; Culley et al., 2016; Hui et al., 2018). For example, flexible plans may respond to  
 46 hydrologic shifts, like a climate trending drier (Kumar et al., 2013), or changing societal values,  
 47 such as a focus towards sustainability and ecological benefits (Kermisch & Taebi, 2017).  
 48 Flexible plans also have downsides. They require identifying signs of system vulnerability  
 49 (Dewar et al., 1994; Haasnoot et al., 2013) to trigger adaptations (Walker et al., 2001), which  
 50 assumes that we can identify a reliable signpost for when to adapt. This may not be the case in  
 51 many systems (Raso et al., 2019). Flexible plans also are expensive and may require additional  
 52 costs for monitoring systems or repetitive structural elements to allow for future adaptations  
 53 (Moore & McCarthy, 2010; Spiller et al., 2015; Walters, 1997).

54 How much we can learn about uncertainty in the future informs whether a flexible  
 55 approach is favorable. To take a flexible approach, we must have an iterative process where new  
 56 information becomes available, the system processes that information, and then changes  
 57 accordingly (Pahl-Wostl, 2007). In this context, the value of learning depends on how much new  
 58 information improves decision making (Williams, 2011). We categorize learning mechanisms, or  
 59 types of information integration, through which we can learn. One mechanism is *learning by*  
 60 *model improvement*, where epistemic uncertainty is improved through the development of better

61 models (Walters, 1997; Williams & Brown, 2016). This type of learning reduces uncertainty  
 62 through the improved understanding of physical and socioeconomic processes. Another  
 63 mechanism is *learning by active information incorporation*, by seeking out and including  
 64 additional sources of information. Examples include developing and incorporating short- and  
 65 long-term precipitation forecasts (Zaniolo et al., 2021) and developing new groundwater  
 66 monitoring systems (Storek et al., 1997). A last mechanism is *learning by observation*, in which  
 67 monitoring of relevant system variables, such as climate trends, are used to update future  
 68 projections (Conroy et al., 2011; Ekholm, 2018; Giuliani et al., 2019; Pulwarty & Melis, 2001).  
 69 In learning by observation, the ability to learn is informed by how correlated near-term  
 70 observations are with long-term trends. For example, if near-term and long-term trends are  
 71 highly correlated, observing an upward trend in a climate variable in recent years indicates a  
 72 long-term upward trend in the future. In this case, ongoing climate observations reduce future  
 73 climate uncertainty, and the climate has a high learning rate. Conversely, when the correlation is  
 74 low, a recent trend does not indicate a future long-term trend, future climate uncertainty remains  
 75 unchanged, and learning does not occur, or occurs slowly.

76 Within water supply planning models focused on climate change uncertainty, most  
 77 planning approaches do not account for learning about uncertainty. Global climate models (or  
 78 general circulation models; GCMs) provide the best available projections for future climate  
 79 conditions. Planning models often use ensembles of different GCMs to simulate system  
 80 performance under uncertainty and identify approaches that perform well across plausible future  
 81 scenarios (Brown & Wilby, 2012; Lamontagne et al., 2018; Quinn et al., 2020; Steinschneider et  
 82 al., 2015). This approach uses a static representation of uncertainty, in which the range of  
 83 plausible futures identified at the outset remain plausible throughout the planning period.  
 84 However, it may be possible to refine the likelihood of future projections as new observations  
 85 become available (Abramowitz & Bishop, 2015; Massoud et al., 2020; Sanderson et al., 2017;  
 86 Urban et al., 2014; Urban & Keller, 2010). Bayesian Model Averaging (BMA) has been used to  
 87 determine the influence of multiple climate models on future aggregated projections based on  
 88 observational data (Duan & Phillips, 2010; Gibson et al., 2019; Massoud et al., 2020). BMA  
 89 develops a set of updated climate projections by averaging prior estimates from the different  
 90 climate models based on how well each model captures historical observations.

91 In the water resources literature, closed loop planning approaches have been used to  
 92 explicitly incorporate learning to inform decision making over time. Closed loop planning  
 93 approaches include multiple classes of methods, including policy search and dynamic  
 94 programming (Herman et al., 2020). Policy search approaches use simulation-based optimization  
 95 to find a decision policy that minimizes a given objective function (see, e.g., Giuliani et al.,  
 96 2016). Policy search has been paired with learning by active information incorporation through  
 97 the addition of exogenous information to condition policy decisions. More informed policies  
 98 generally result in improved policy outcomes (e.g., Giuliani et al. 2019; Woodward, Kapelan,  
 99 and Gouldby 2014). Policy search methods have been used in flood (Ceres et al., 2022; Kwakkel  
 100 et al., 2015, 2016; Woodward et al., 2014) and urban water supply (Mortazavi-Naeini et al.,  
 101 2015; Paton et al., 2014; Zeff et al., 2016) infrastructure planning.

102 One benefit of dynamic programming is that new information can be explicitly  
 103 incorporated at each time step using a prescribed probability distribution, and the problem  
 104 formulation incorporates all potential future information in determining the optimal planning  
 105 decisions (Fletcher, Lickley, et al., 2019; Giuliani et al., 2016). Dynamic programming and

106 optimization methods with Bayesian updating frameworks have been used in flood (Doss-Gollin  
107 & Keller, 2022; Hui et al., 2018) and flexible water (Fletcher, Lickley, et al., 2019) infrastructure  
108 planning problems. Jeuland & Whittington (2014) use decision trees, which use dynamic  
109 programming as solution method but do not make the Markov assumption typical in larger  
110 problems, within an engineering options analysis simulation framework to systematically  
111 evaluate infrastructure selection, sizing, and sequencing. Fletcher, Lickley, and Strzepek (2019)  
112 develop the first planning framework to explicitly incorporate learning about climate change  
113 uncertainty into the upfront flexible infrastructure planning decision. They use Bayesian  
114 modeling (Smith et al., 2009) to develop future temperature and precipitation uncertainty  
115 projections and use learning by observation of the climate state to compare flexible and static  
116 infrastructure planning approaches. However, this work did not test how different climate  
117 learning rates impact costs and planning decisions to understand the conditions under which  
118 flexible water infrastructure is most valuable.

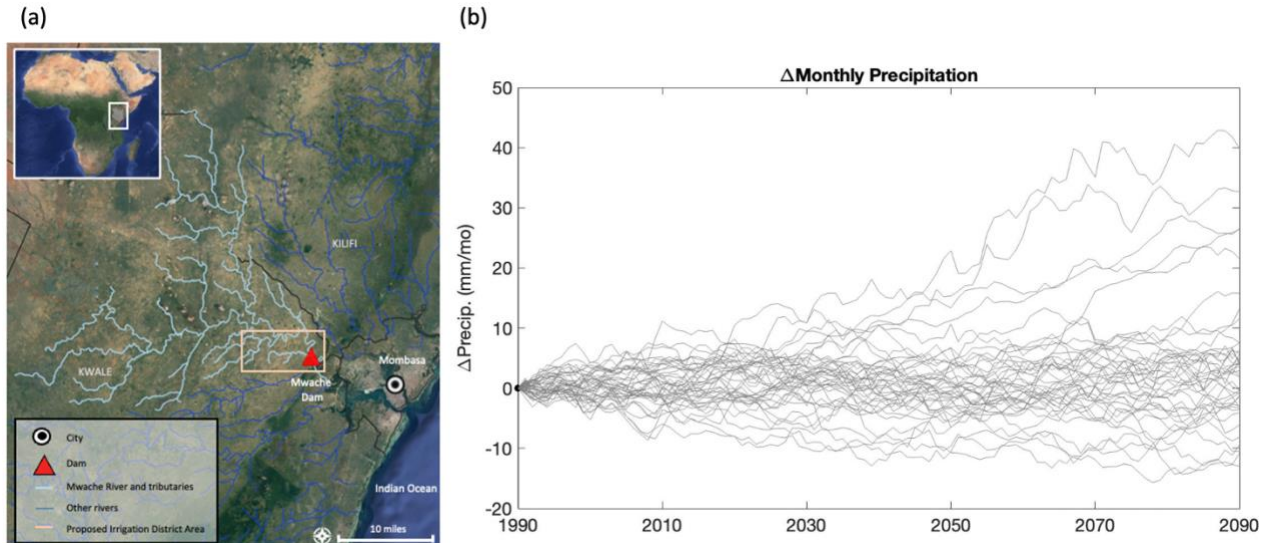
119 This gap is the motivation for our current work. We develop a framework to assess how  
120 differences in the amount of learning about climate uncertainty affect the value of flexible water  
121 infrastructure in providing low-cost, reliable water supply. One key contribution is the use of  
122 information theory metrics to quantify uncertainty changes. We demonstrate this framework on a  
123 stylized dam planning case study. To assess the effect of variable learning rates, we design future  
124 climate scenarios with different rates of learning by observation using an exploratory Bayesian  
125 modeling approach. Then, we develop an approach to quantify the impacts of learning about  
126 climate change uncertainty on flexible and static infrastructure designs. We demonstrate this  
127 framework on the Mwache Dam near Mombasa, Kenya. GCMs in this region have diverging  
128 future precipitation projections with long-term uncertainty on whether this area will become  
129 wetter or drier. We find that a high-learning climate often increases the value of flexibility and  
130 better avoids over- or underbuilding infrastructure compared to a low-learning climate. We also  
131 find that flexible infrastructure is most valuable under wet climate conditions by avoiding  
132 overbuilding.

## 133 2 Methods

### 134 2.1 Case study: Mwache Dam in Mombasa, Kenya

135 We apply our framework to the Mwache Dam near Mombasa, Kenya. The Mwache Dam  
136 site, Mwache River, and associated tributaries are shown in Figure 1a. The dam is about 22  
137 kilometers west of Mombasa, Kenya. The dam's main purposes are to meet water supply for  
138 growing urban and agricultural demands in the region. Over the next 15 to 20 years, urban water  
139 demands are expected to double in Mombasa (Ojwang et al., 2017). Additionally, as part of the

140 infrastructure project, planned irrigation districts will receive water from the dam (State  
 141 Department of Natural Water Services, 2016), as highlighted on the map.



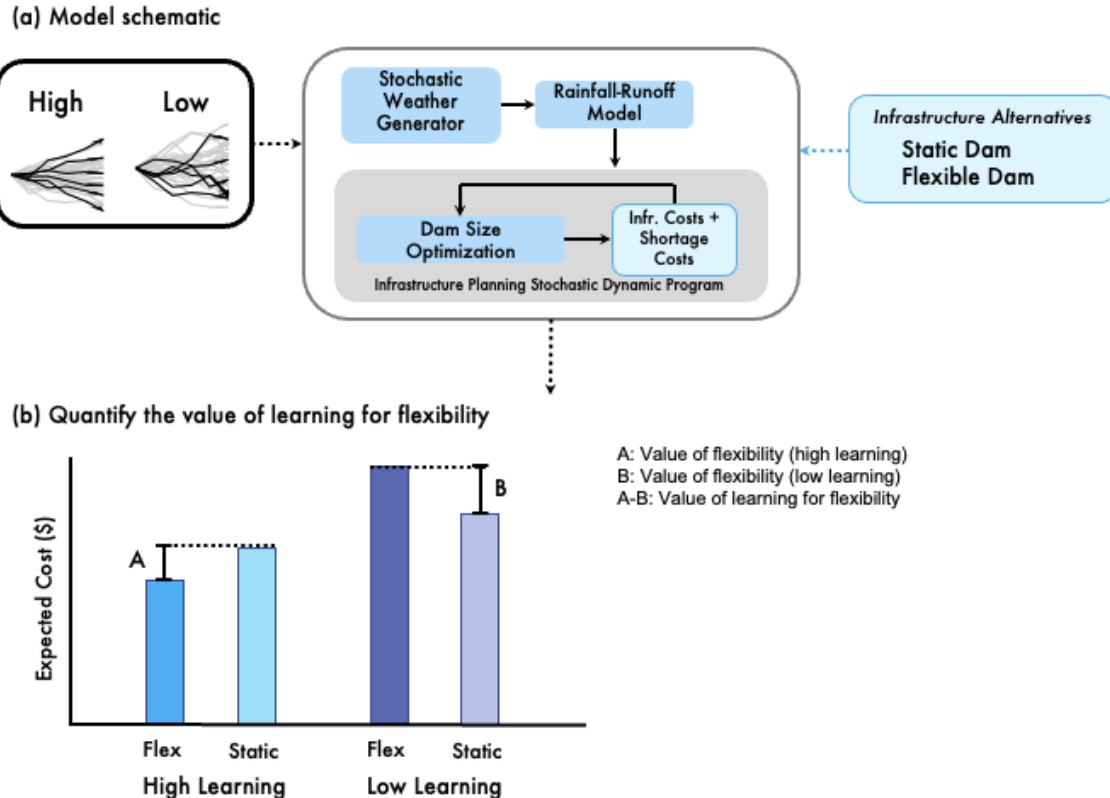
142  
 143 *Figure 1. Case study location. a) Map of Mwache River and tributaries, b) RCP4.5 and RCP8.5 GCM*  
 144 *projections for 20-year precipitation moving averages near Mombasa, Kenya.*

145 Figure 1b shows the projected precipitation change in Mombasa relative to a 1990  
 146 baseline under 21 GCMs for RCP4.5 and RCP8.5 emissions pathways. Table S1 in the  
 147 Supplementary Information (SI) includes the full GCM list. The diverging trend for different  
 148 GCMs highlights the large uncertainty in future precipitation trends in this region due to climate  
 149 change. This diverging trend challenges water supply planning and motivates the use of flexible  
 150 water infrastructure to avoid over- or underbuilding.

151 **2.2 Framework Overview**

152 We develop a novel framework to assess how different rates of learning about  
 153 precipitation affect the value of flexible infrastructure in low-cost, reliable water supply. Our  
 154 approach has three key steps, illustrated in Figure 2. First, in panel a, we develop two contrasting  
 155 climate learning scenarios: a high-learning climate scenario where new observations are  
 156 correlated with past observations and substantially reduce future uncertainty, and a low-learning  
 157 climate scenario where new observations are uncorrelated and therefore less informative. In  
 158 parallel, we design two infrastructure alternatives: a static dam that cannot be modified once  
 159 built, and a flexible dam that can be expanded at most once during the planning period. Second,  
 160 we develop an infrastructure planning model using stochastic dynamic programming (SDP)  
 161 (hereafter termed infrastructure planning SDP) to evaluate the infrastructure and shortage costs  
 162 of the optimized static and flexible dam alternatives in the high- and low-learning climate  
 163 scenarios. We use a 100-year time horizon with new climate information incorporated and  
 164 actions updated every 20 years. Finally, in panel b, we use these results to quantify the value of  
 165 flexibility, defined as the cost savings of the flexible dam compared to the static dam. We then  
 166 quantify the value of learning for flexibility, defined as the difference in the value of flexibility  
 167 in the high-learning climate compared to the low-learning climate. This framework allows us to

168 assess the interaction between learning about climate uncertainty and infrastructure flexibility,  
 169 and to quantify the degree to which greater learning improves the value of flexible planning.



170  
 171 *Figure 2. Schematic illustrating framework for quantifying the value of learning about climate uncertainty for*  
 172 *flexible water infrastructure*

### 173 2.3 Designing Climate Learning Scenarios

174 First, we develop climate learning scenarios that model learning by observation using  
 175 exploratory Bayesian updating, in which we systematically adjust the likelihood function to  
 176 change the influence of new observations on the posterior. In our exploratory Bayesian model,  
 177 the prior distribution reflects the full range of uncertainty in future precipitation projections at the  
 178 outset of the planning period. As the planning period goes on, more data about how precipitation  
 179 is changing becomes available, which is used to update the prior and develop a posterior  
 180 distribution. The difference between the posterior and prior distributions reflects what is learned  
 181 about uncertainty from the new data. Here the new data is synthetic data that corresponds to  
 182 simulated precipitation in the infrastructure planning model.

183 We design two scenarios, a high-learning climate and a low-learning climate. In the high-  
 184 learning climate scenario, new observations have a large influence on the prior, leading to a  
 185 posterior that substantially narrows around the new data. In the low-learning climate scenario,  
 186 new observations have a limited effect, and the posterior more closely resembles the prior,  
 187 reflecting slow learning. In Bayes' theorem, the likelihood function controls the degree to which  
 188 the posterior is changed by new data. Therefore, we design the high- and low-learning climate  
 189 scenarios by developing likelihood functions with low and high variance, respectively. In  
 190 previous work that integrates climate model projections with observational data (e.g. Smith et al.

191 2009), the likelihood function describes the error between observed and modeled projections of  
 192 precipitation change. Models with larger historical errors have likelihood functions with higher  
 193 variance terms, leading to less influence on the posterior. Here, as an exploratory approach to  
 194 vary the amount of learning, we directly manipulate the variance of the likelihood function to  
 195 control the amount of influence the new synthetic observation has on the posterior.

196 Our Bayesian model is presented in Equation 1. We model a single period update, where  
 197 precipitation change in time  $t$  is used to update the projection for precipitation in  $t+1$ . This choice  
 198 is made to align with the formulation of our stochastic infrastructure planning model, which uses  
 199 single-period Markov state transitions. We develop projections to the end of the planning period  
 200 by applying Monte Carlo simulation to the single period transitions. We use a normal-normal  
 201 conjugate model for the single period update. The assumption of normality aligns with previous  
 202 work modeling precipitation change (Ruosteenoja et al., 2007) and is validated using a  
 203 Kolmogorov-Smirnov (K-S) test. The K-S test results are listed in SI Section S2.

204 In  $t=1$ , the model is:

$$\begin{aligned}
 205 \quad P(\Delta p_1) &\sim N(\Delta p_0, \sigma_0^2) && \text{(Prior in } t=1) \\
 206 \quad P(\Delta p_0 | \Delta p_1) &\sim N(c_l \Delta p_0, \alpha_l) && \text{(Likelihood in } t=1) \\
 207 \quad P(\Delta p_1 | \Delta p_0) &\sim N(\mu_1 \Delta p_0, \nu_1 \sigma_0^2) && \text{(Posterior in } t=1) \\
 208 \quad \text{where } \mu_1 &= \frac{c_l * \sigma_0^2 + \alpha_l^2}{\sigma_0^2 + \alpha_l^2}, \quad \nu_1 = \frac{\alpha_l^2}{\sigma_0^2 + \alpha_l^2}
 \end{aligned}$$

209 *Equation 1*

210 This model uses a recursive approach in which the posterior from one time period becomes the  
 211 prior in the next; in the  $t=1$  model,  $\Delta p_0$  is the “synthetic observation” i.e. precipitation change in  
 212 the previous ( $t=0$ ) period that is used to update estimated precipitation change in the current ( $t=1$ )  
 213 period.

214 Using the same single-period likelihood function,  $P(\Delta p_{t-1} | \Delta p_t) \sim N(c_l \Delta p_{t-1}, \alpha_l)$ , we  
 215 derive the general posterior for any time period:

$$\begin{aligned}
 216 \quad P(\Delta p_t | \Delta p_{t-1}, \dots, \Delta p_0) &\sim N(\mu_t \Delta p_{t-1}, \nu_t \sigma_0^2) \quad \forall t \geq 0 \\
 217 \quad \text{where } \mu_t &= \frac{t * c_l \sigma_0^2 + \alpha_l^2}{t * \sigma_0^2 + \alpha_l^2}, \quad \nu_t = \frac{\alpha_l^2}{t * \sigma_0^2 + \alpha_l^2}
 \end{aligned}$$

218 *Equation 2*

219 We define the terms in this model as follows.  $\Delta p_t$  is the change in precipitation ending in  
 220 time  $t$  relative to the current time period,  $t=0$ .  $\sigma_0^2$  is the variance of the prior in  $t=0$ , reflecting  
 221 current knowledge of precipitation change uncertainty. We define the mean of the likelihood  
 222 using a multiplicative shifting factor,  $c_l$ , which controls the lag-1 autocorrelation in  $\Delta p$ . The  
 223 subscript  $l$  refers to the climate learning scenario, which can be high ( $l = H$ ) or low ( $l = L$ ).  $c_l$   
 224 is greater in the high-learning scenario than the low-learning scenario, representing the  
 225 correlation between near-term observations and long-term change.  $\alpha_l$  is the variance of the  
 226 likelihood, where higher values are analogous to greater error between climate models and  
 227 observations, leading to lower learning by observation.  $c_l$  and  $\alpha_l$  are parameters we manipulate  
 228 directly for exploratory analysis. Together, they control the amount of learning, with  $c_l$   
 229 determining how correlated near-term precipitation is with long-term precipitation, and  $\alpha_l$

230 determining how much the new observation affects the prior estimate. Finally,  $\mu_t$  and  $\nu_t$  are  
 231 derived using the normal-normal conjugate (Marin & Robert, 2007).

232 The numerical values of these parameters are given in Table 1.  $\sigma_0^2$  was chosen to be  
 233 comparable to the variance of one-period changes in precipitation in the ensemble of GCM  
 234 projections in Mombasa.  $c_l$  and  $\alpha_l$  were chosen with two goals. First, we choose higher  $c_l$  and  
 235 lower  $\alpha_l$  in the high-learning scenario compared to the low-learning scenario, reflecting greater  
 236 autocorrelation and greater updating based on new information, both of which lead to more  
 237 learning. Second, we want the end-of-century prior precipitation distributions to be the same and  
 238 comparable to the mean and variance across GCM projections. This ensures that the difference in  
 239 the scenarios reflect differences in learning rather than differences in precipitation trends or  
 240 initial uncertainty. The method used is discussed in SI Section S3.

241 *Table 1. High- and Low-Learning Climate Scenario Parameters*

Learning scenario	$\sigma_0$	$c_l$	$\alpha_l$
High	5.0	1.15	2
Low	5.0	-0.58	50

242

243 

## 2.4 Quantifying Learning

244 The previous section described our approach to designing scenarios that reflect high and  
 245 low rates of learning by observation about climate uncertainty. Here, we quantify the amount of  
 246 learning in each model simulation. This serves two purposes. First, it allows us to validate that  
 247 the approach to design high- and low-learning climate scenarios does indeed lead to differences  
 248 in learning. Second, it allows us to quantify the amount of learning across different model  
 249 simulations, which we use to assess the impact of different amounts of learning on flexibility.  
 250 We quantify the change in predicted precipitation distributions using KL divergence, an  
 251 information theory metric that measures the amount of information gain through comparing two  
 252 distributions (Kullback & Leibler, 1951). The KL divergence between the posterior and prior in a  
 253 Bayesian model is commonly used to measure the amount of learning from new observations  
 254 (Gelman et al., 2021). Previous climate science and water resources work uses KL divergence to  
 255 compare synthetic climate projections, such as precipitation or streamflow, with observed data  
 256 (e.g., Leung and North 1990; Nearing and Gupta 2015; Weijs, Schoups, and van de Giesen  
 257 2010).

258 Here we use KL divergence to quantify the amount of learning by observation in  
 259 probabilistic precipitation change projections. We apply Monte Carlo simulation to our Bayesian  
 260 model for single period transitions (Equations 1 and 2) to develop probabilistic precipitation  
 261 change projections starting in our initial time period (1990;  $t=0$ ) through the end of our modeled  
 262 planning period (2090;  $t=5$ ) with a time step of 20 years. We vary the number of recursive  
 263 Bayesian updates corresponding to how many years of new precipitation observations are used  
 264 for learning. We define our prior as the information available in 1990 ( $t=0$ ). Then we can  
 265 develop a posterior for any future time period  $t$  based on new observations between time 0 and  $t-1$ . For example, we can simulate precipitation distributions for the year 2090, using observations  
 266 through the year 2070; this requires simulation through four Bayesian updates, each  
 267 corresponding to a new 20-year average observation. In this example, we define 1990 as the

269 prior year, 2070 as the information year, and 2090 as the projection year. Further, we propagate  
 270 uncertainty through our simulation model using Monte Carlo simulation to develop analogous  
 271 projections and updates for water shortages in addition to precipitation. We apply KL divergence  
 272 to calculate learning between prior and posterior projections using a distribution of precipitation  
 273 or water shortage predictions. For discrete distributions, this is calculated as shown in Equation  
 274 3:

$$275 \quad D_{KL}(P_{t,i} \| P_{t,p}) = \sum_{x \in X} P_t(x) * \log \frac{P_{t,i}(x)}{P_{t,p}(x)},$$

276 *Equation 3*

277 where  $P_{t,i}(x)$  is the probability distribution for precipitation (or water shortages) in projection  
 278 year  $t$  based on observations between  $t=0$  and information year  $i$ , and  $P_{t,p}(x)$  is the probability  
 279 distribution at projection year  $t$ , based only on information from prior year  $p$ .  $x$  is a discrete  
 280 random variable representing possible values of future precipitation (or water shortages). A  
 281 discrete formulation was chosen to align with the infrastructure planning SDP, which constrains  
 282 precipitation (and water shortage) values to discretized increments; see below. We follow  
 283 recommendations from Gong et al. (2014) for applying KL divergence to precipitation and water  
 284 availability data. See SI Section S4 for details.

285 **2.5 Infrastructure Planning Model using Stochastic Dynamic Programming**

286 After developing the climate learning scenarios and an approach to quantify the learning  
 287 in each, we now develop an infrastructure planning model that uses SDP to optimize and  
 288 compare the performance of static and flexible infrastructure alternatives under the contrasting  
 289 climate learning scenarios. The infrastructure planning SDP identifies the least-cost  
 290 infrastructure planning policy under climate uncertainty over a 100-year time horizon with 20-  
 291 year time steps. Climate uncertainty is incorporated into the infrastructure planning SDP by  
 292 defining a state variable that represents average precipitation in each 20-year period. We use the  
 293 Bayesian model from Equations 1 and 2 to characterize the transition probabilities for the  
 294 precipitation state variable. The current precipitation state in the SDP is used as the synthetic  
 295 data  $\Delta p_t$  in the Bayesian model. The transition probabilities that lead to future precipitation states  
 296 therefore reflect what is learned from the current state as an observation. This approach  
 297 integrates learning by observation into optimal infrastructure planning policies. This approach  
 298 was developed and applied in Fletcher, Lickley, and Strzepek (2019) and Fletcher et al. (2019).  
 299 We formulate and solve the infrastructure SDP using the Bellman equation (Bellman, 1954) as  
 300 follows:

$$301 \quad V_t(s_t) = \underset{a \in A}{\operatorname{argmin}} \quad C(s_t, a_t, t) + \gamma * \sum_{s \in S} P(s_{t+1} | s_t, a) * V_{t+1}(s_{t+1})$$

302 *Equation 4*

303 where  $t \in \{1, \dots, 5\}$  for 20-year planning periods from  $t=1$  representing 2001-2020 to  $t=5$   
 304 representing 2081-2100.  $S$  is the state space, comprising state variables  $S^P$  for the precipitation  
 305 state, which ranges from 49 to 119 millimeters per month in discretized one-millimeter bins, and

306  $S^Z$  for the infrastructure state, which comprises the static dam, flexible dam unexpanded, or  
 307 flexible dam expanded to multiple candidate sizes.  $A$  is the set of actions: what dam to construct  
 308 in the first time period, and if and how much to expand the flexible dam in later time periods.  $C$   
 309 is the cost function comprising capital costs and water shortage costs, and  $V$  is the value  
 310 function, the lowest cost in each state and time.  $\gamma$  is the discount rate; we include scenarios for  
 311 0% and 3%. A 3% discount rate is commonly used in climate change analysis work on  
 312 infrastructure development in Africa (Cervigni et al., 2015). Zero discounting was chosen as a  
 313 contrasting example where there is no preference for the present over the future. This allows us  
 314 to isolate the value of flexibility in addressing uncertainty from the value of flexibility driven by  
 315 discounting, which incentivizes the delay of capital costs.  $P$  is the transition probability of  
 316 transitioning to a given future state  $s_{t+1}$  in the next time period based on the current state  $s_t$  and  
 317 our action  $a$ . The transition probabilities for state vectors  $S^P$  and  $S^Z$  are independent, where the  
 318 precipitation transition probabilities are defined by the Bayesian model as described above and  
 319 the infrastructure state transitions are deterministic and defined by the actions. We solve for the  
 320 optimal policies and value function using backwards recursion.

321 The shortage cost component of the cost function is developed using a water resource  
 322 system model that applies stochastic weather generation to the current precipitation state,  
 323 generating monthly precipitation time series that force a rainfall-runoff model, which in turn  
 324 forces a reservoir operations model and estimates shortages relative to demand. Shortage costs  
 325 are assumed proportionate to the square deficit of water shortages. The approach follows  
 326 Fletcher, Lickley, and Strzepek (2019) with minor improvements. Notably, operating policies are  
 327 updated over time as the climate changes instead of using a fixed rule curve approach. Details on  
 328 each model component are available in SI Sections S5-S8.

329 The infrastructure component of the cost function and the actions models two  
 330 infrastructure alternatives: a static and flexible dam. Both dams are built at the start of the  
 331 planning period and use an existing cost model based on reservoir volume. The static dam uses  
 332 economies of scale through building a larger dam upfront that cannot be changed later in the  
 333 planning period. In contrast, the flexible dam is built small initially, but has multiple expansion  
 334 options that can be used once in the planning period, albeit for additional costs. Hence,  
 335 expanding the flexible dam to an equivalent size of the static dam is more expensive, and so  
 336 flexibility is traded off with economies of scale. Detailed cost model information is in SI Section  
 337 S9.

338 We combine the high- and low-learning transition probabilities with the static and  
 339 flexible infrastructure alternatives in our infrastructure planning SDP to obtain the optimal, i.e.,  
 340 lowest expected total cost, static and flexible infrastructure designs under our two climate  
 341 learning scenarios. Then, we re-run our infrastructure planning SDP using the previously  
 342 determined infrastructure designs to obtain the optimal dam policies, which includes whether to  
 343 choose the static or flexible dam initially, and if we choose the flexible dam, if, when, and by  
 344 how much to expand the dam's capacity under our discretized state space.

345 Lastly, we use Monte Carlo simulation to test how the optimal dam designs and policies  
 346 perform on cost and reliability metrics under our two climate learning scenarios. Through  
 347 simulating 10,000 instances of possible time series of precipitation from the climate learning  
 348 scenarios, and applying the optimal policies from the SDP, we develop distributions of the costs,

349 reliability, and infrastructure planning decisions. To explore how the dynamics of learning and  
350 flexibility change under different climate simulations, we categorize the simulations into dry,  
351 moderate, or wet based on their end of century precipitation values. Details available in SI Figure  
352 S2.

## 353 2.6 Quantifying the Value of Learning for Flexibility

We quantify the value of learning for flexibility to understand how differences in learning about climate uncertainty affect the value of flexible water infrastructure. A high-learning climate may increase the value of flexibility because dry or wet climate simulations are more likely to continue in that direction, so optimal dam expansion decisions can be made earlier. Since the planning cost of a particular climate learning scenario is influenced by natural climate variability, e.g., how wet or dry the climate is, as well as how much it is possible to learn about the climate, we isolate the value of learning from climate variability. To understand the differences between high- and low-learning climate scenarios, we compare the costs of the flexible and static dams under the two climate learning scenarios, as shown in Figure 2b.

363 We quantify the value of learning for flexibility as the difference between the expected  
 364 costs of the static and flexible dams under high- and low-learning scenarios, as shown in  
 365 Equation 5:

369 This value is positive when static dam costs exceed flexible dam costs, as shown in  
370 Figure 2b.

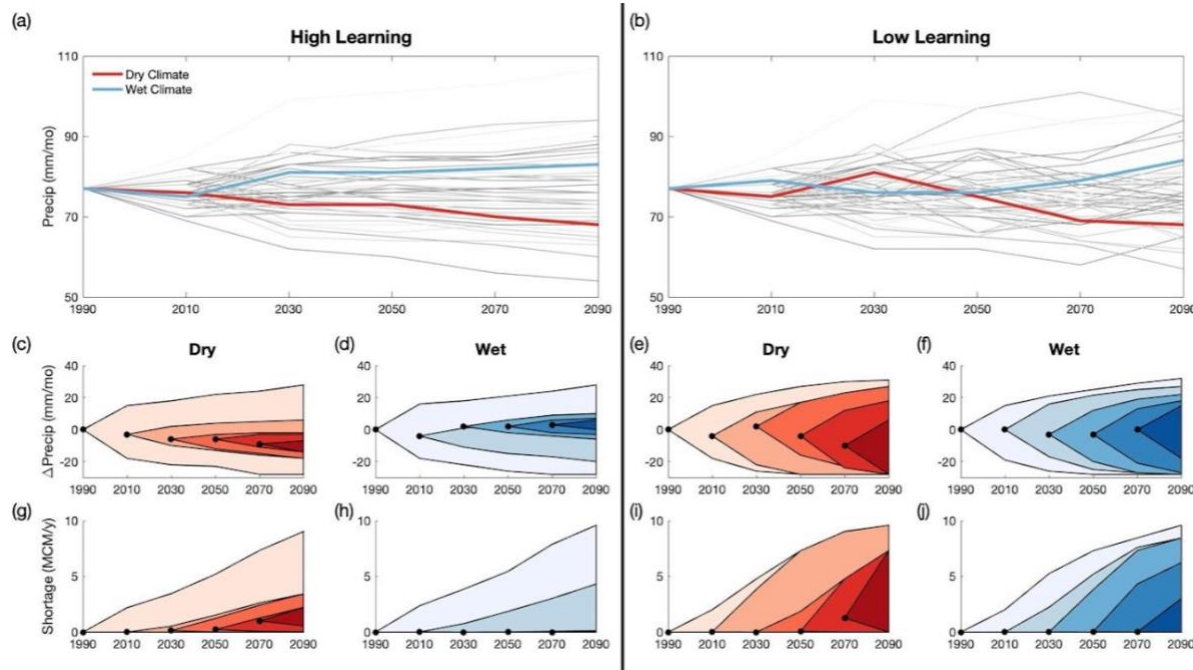
372 **3 Results**

373 First, we present results from the exploratory Bayesian model for the high- and low-  
374 learning climate scenarios. Then, we present the results on the dam infrastructure decisions and  
375 costs using the infrastructure planning SDP for each climate learning scenario.

### 3.1 High- and Low-Learning Climate Scenarios

377 Figure 3 presents results from the exploratory Bayesian model, illustrating differences in  
 378 simulated precipitation time series and learning rates between the high- and low-learning climate  
 379 scenarios. This illustrates how new synthetic observations reduce uncertainty in long-term  
 380 precipitation projections more with high-learning climates than low-learning climates. In panel a,  
 381 under high learning, a drying or wetting trend in simulated precipitation near the beginning of the  
 382 time series is likely to continue to end of century. In contrast, in panel b we see that under low  
 383 learning, early trends do not always continue. We measure this using average one-lag

384 autocorrelation values, which are 0.43 and 0.19 for high- and low-learning climate scenarios,  
 385 respectively.

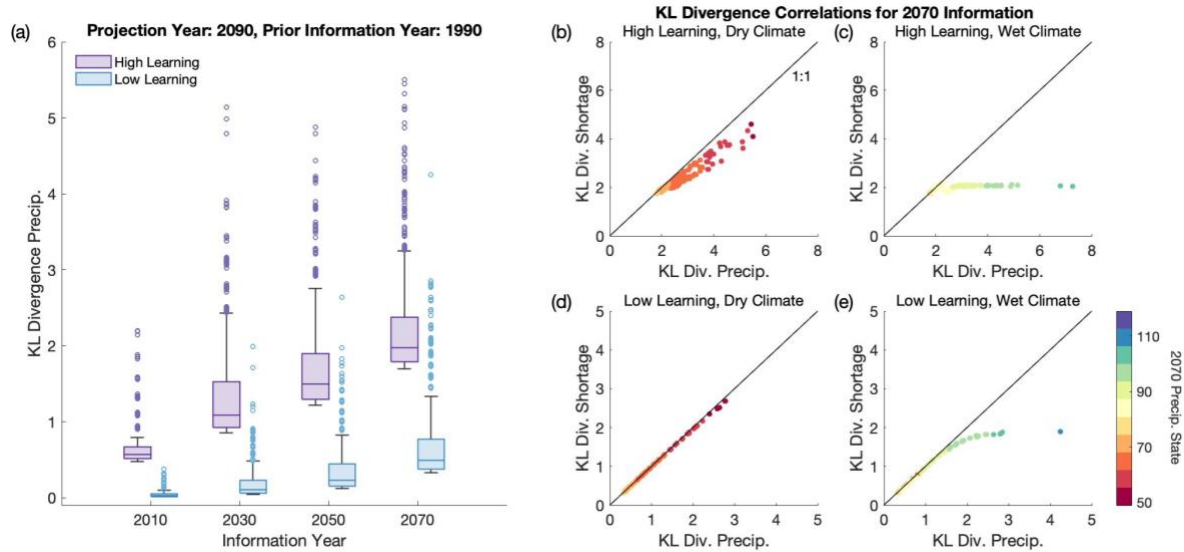


386  
 387 *Figure 3. High- and low-learning climate sample precipitation and water shortage simulations. Sample simulations*  
 388 *are shown for wet and dry realizations, defined by their end-of-century precipitation change. a-b) Sample*  
 389 *precipitation simulations under high- and low-learning climate scenarios are shown in gray. Red and blue lines*  
 390 *indicate samples shown in c-j. c-f) Sample precipitation instances with uncertainty bounds under high- and low-*  
 391 *learning, dry and wet climate simulations. g-j) Sample water shortage instances with uncertainty bounds under*  
 392 *high- and low-learning, dry and wet climate conditions. The specific simulation values are shown by the black*  
 393 *points. As the shading gets darker, the observation time period progresses through the 21<sup>st</sup> century.*

394 In panels c-f, we illustrate learning by observing precipitation uncertainty over time. In  
 395 each panel, we simulate one precipitation time series, use it in the Bayesian model to update later  
 396 projections, and show the resulting posterior distributions. In panels g-j, we show how this  
 397 process propagates through the infrastructure model and leads to learning about shortage  
 398 uncertainty, which is the metric we ultimately care about to meet water demands. High learning  
 399 leads to large reductions in uncertainty in both precipitation and water shortages (panels c-d, g-  
 400 h). In contrast, low learning leads to smaller reductions in precipitation uncertainty (panels e,f),  
 401 but the impact on water shortage uncertainty varies across dry and wet simulations. Uncertainty  
 402 in water shortages is reduced modestly in dry simulations (panel f) and greatly in wet simulations  
 403 (panel j). This demonstrates a non-linear relationship between precipitation and water  
 404 availability: above a certain precipitation threshold, enough water is available, and no water  
 405 shortages incur. Since Figure 3 illustrates the dynamics of updating uncertainty using one  
 406 realization of a time series, the optimization and simulation results, which use many realizations,  
 407 are unchanged by the choice of time series here. SI Figure S3 highlights contrasting low-learning  
 408 dry and wet realizations for reference.

409 Next, we use KL divergence to quantify the learning from additional precipitation  
 410 observations, shown in Figure 4. The results confirm that the high-learning climate scenario  
 411 leads to greater KL divergence values in simulated precipitation compared to low learning. The

412 boxplots in panel a show the range of KL divergence values for simulated precipitation under  
 413 high- and low-learning climate scenarios for different information years, using 1990 as the prior  
 414 year and 2090 as the projection year. The distribution of KL divergence values is higher in the  
 415 high-learning climate scenarios across all information years compared to the low-learning  
 416 climate scenarios.



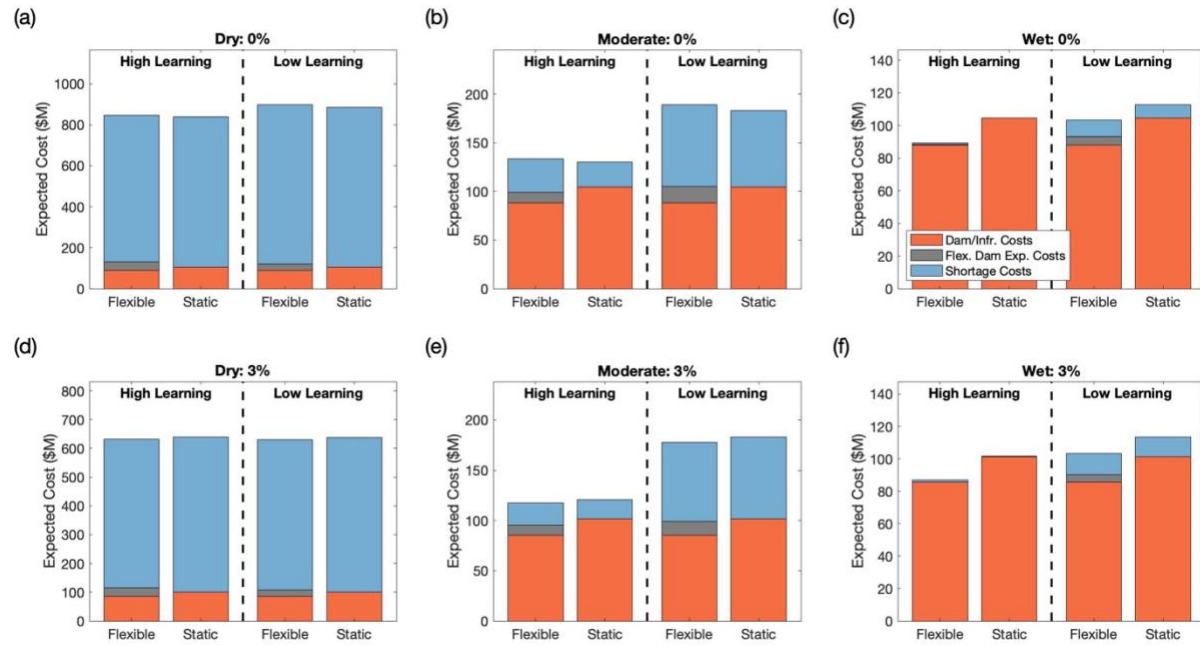
417  
 418 *Figure 4. KL divergence results for high- and low-learning, wet and dry climate scenarios. A) Distributions of KL*  
 419 *divergence values for precipitation across different information years for a prior information year of 1990 and a*  
 420 *projection year of 2090. b-e) Correlations between KL divergence for precipitation and water shortages. The black*  
 421 *lines show a 1:1 line for reference, and the points are colored by the 2070 precipitation state, which is the*  
 422 *information year used here.*

423 Panels b-e show the relationship between KL divergence values for precipitation and  
 424 water shortages, and see how this relationship changes in high- vs. low-learning climates and wet  
 425 vs. dry simulations. In wet simulations (panels c, e) KL divergence is sometimes lower for water  
 426 shortages than for precipitation. Since water shortages do not occur in many wet simulations, the  
 427 distributions of water shortage uncertainty have a low expected value, exhibit a small amount of  
 428 uncertainty, and do not change much with additional observations. New information about  
 429 precipitation and water availability is not valuable in this situation. In comparison, under a dry  
 430 climate, the KL divergence values for water shortage have a linear correlation with the KL  
 431 divergence values for precipitation, as seen by comparing the scatter plots to the black line with a  
 432 slope of one. Therefore, under a dry climate we learn similar amounts about precipitation and  
 433 water shortages.

434       3.2 Dam Infrastructure Decisions and Costs under High- and Low-Learning Climate  
 435       Scenarios

436 After presenting our climate learning scenario results, we now explore the performance  
 437 of the dam infrastructure alternatives for each climate learning scenario. We first quantify how  
 438 high- and low-learning climates influence infrastructure decisions and costs across dry,  
 439 moderate, and wet climate simulations and discount rates (Figure 5). The flexible dam is most  
 440 valuable under wet climate simulations, where flexibility prevents overbuilding. Additionally,  
 441 high-learning climate scenarios lead to decreased water shortages and costs in wet and moderate

442 climate simulations because precipitation trends earlier in the planning period are more  
 443 consistent and predictable throughout. However, under dry climate simulations, both high- and  
 444 low-learning climate scenarios have similar water shortage penalty costs. This is because under  
 445 dry climates, learning is not particularly valuable as natural water availability simply does not  
 446 meet demand regardless of the infrastructure decision.



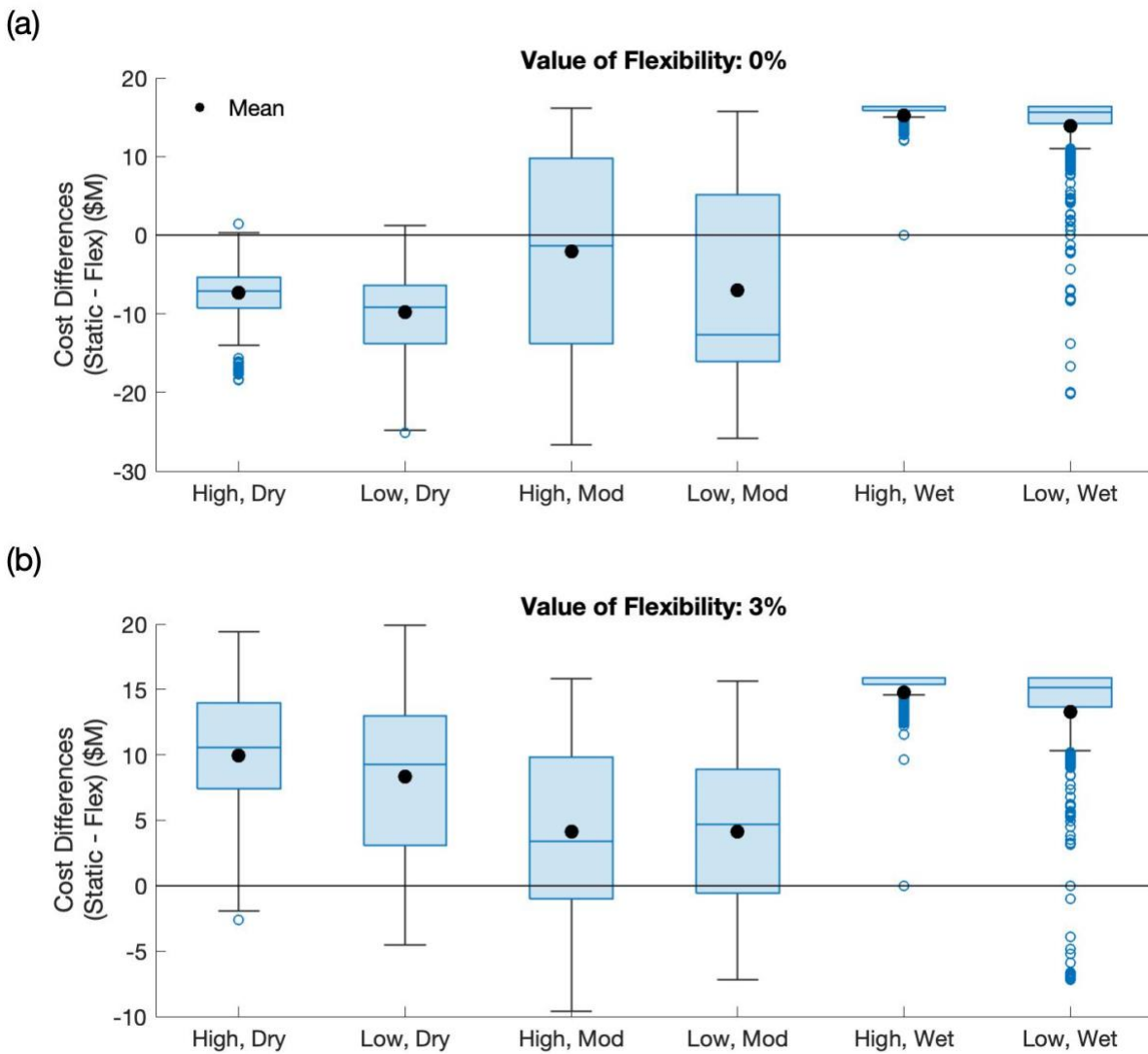
447  
 448 *Figure 5. Expected costs across 10,000 simulations of optimal planning policies for flexible vs. static dams and*  
 449 *high- vs. low-learning climate scenarios. Bars show the portion of the costs associated with dam infrastructure*  
 450 *(orange), dam expansion (gray), and water shortage penalty costs (blue). Costs are compared under 0% (a-c) and*  
 451 *3% (d-f) discount rates; and dry (a, d), moderate (b, e), and wet (c, f) precipitation simulations. The vertical axis*  
 452 *scale varies across panels to facilitate readability of results.*

453 With zero discounting in panels a-c, the expected cost of the flexible dam is less than the  
 454 expected cost of the static dam only for wet climate simulations, where the costs are driven by  
 455 infrastructure costs as water shortage penalty costs are low. The static dam slightly outperforms  
 456 the flexible dam for dry and moderate climate simulations. This is because the additional costs to  
 457 expand the flexible dam are not fully mitigated through decreased water shortage penalty costs.  
 458 There are two main reasons for this. First, since the flexible dam is initially smaller than the  
 459 static dam, drier climate simulations near the beginning of the planning period may lead to larger  
 460 water shortage penalty costs initially. Second, even once the flexible dam expands, lack of water  
 461 availability in drier simulations diminishes the value of increasing the amount of dam storage. SI  
 462 Figure S4 illustrates this result by presenting shortage costs of different dam sizes for different  
 463 precipitation conditions. With a discount rate, investments later in the simulation horizon are  
 464 cheaper. Flexible dams both delay infrastructure design decisions to learn about uncertainty and  
 465 delay investments, which decreases their net present cost. For a 3% discount rate (panels d-f), the  
 466 expected cost of the flexible dam is always less than that of the static dam, though still similar in  
 467 magnitude.

468 Next, we quantify the value of flexibility under high- and low-learning climate scenarios  
 469 and contrasting precipitation simulations. This is seen in Figure 6, which illustrates distributions

470 of the cost difference between flexible and static alternatives under a range of simulations.  
 471 Flexibility is most valuable for wet simulations when water shortage penalty costs are low, and  
 472 we do not need to expand the flexible dam. But many negative outliers occur, especially with a  
 473 low learning climate, where overbuilding is more likely, which occurs when the flexible dam  
 474 expands even though a larger dam is not ultimately needed. Higher discount rates increase the  
 475 value of flexibility. With no discounting in panel a, the value of flexibility is often negative  
 476 under moderate and dry scenarios, although it is less negative under high-learning compared to  
 477 low-learning climate scenarios. With the 3% discount rate in panel b and all climate simulations,  
 478 the distributions for the value of flexibility are mainly positive.

479

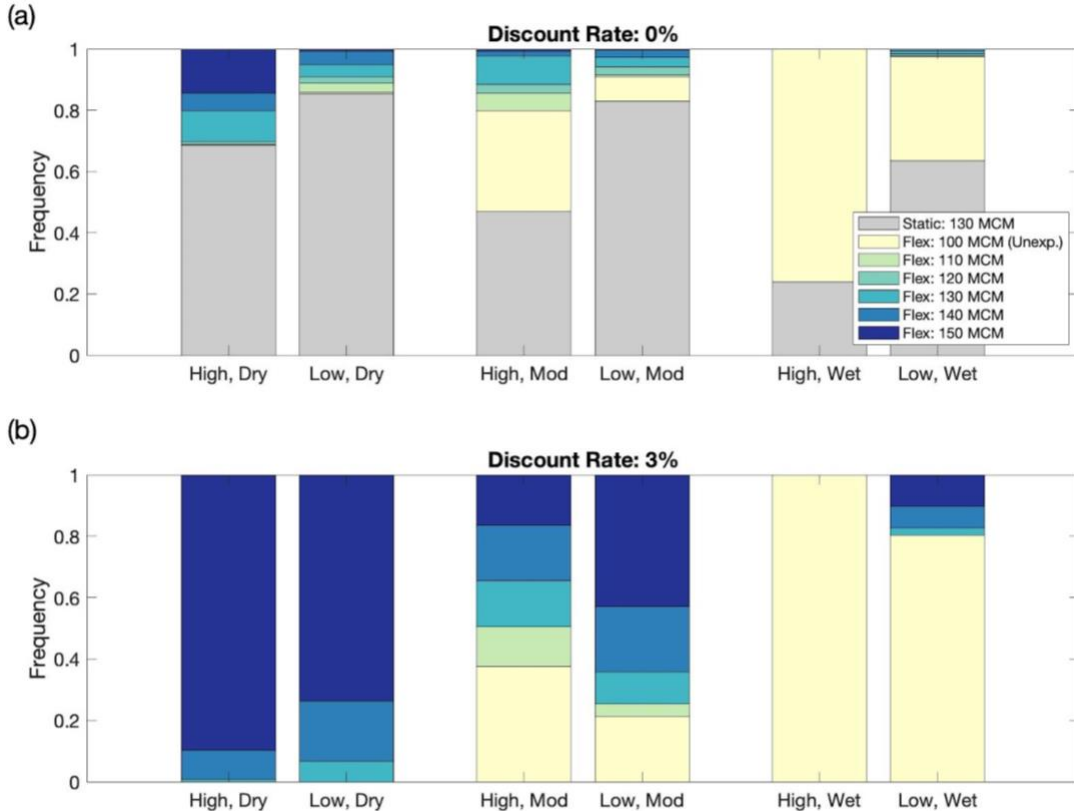


480  
 481  
 482  
 483  
 484

Figure 6. Distributions of the value of flexibility across 10,000 precipitation simulations under a) 0% and b) 3% discount rates. Both panels show the distributions of cost differences between the static and flexible dams under high- and low-learning climate scenarios; and dry, moderate, and wet simulations. The black points show the mean of the distributions.

485 Another interesting result in Figure 6 is that there are different trends in the distributions  
 486 with the 0% and 3% discount rates. With the 3% discount rate in panel b, cost differences

487 between the static and flexible dams are, on average, greater under dry conditions than moderate  
 488 conditions; this is reversed for the 0% discount rate in panel a. An explanation for this is that  
 489 with the 3% discount rate for both high and low learning, a larger fraction of simulations where  
 490 the flexible dam is chosen expand to the 140 or 150 MCM dam, which exceeds the static dam of  
 491 130 MCM, compared to the 0% discount rate.



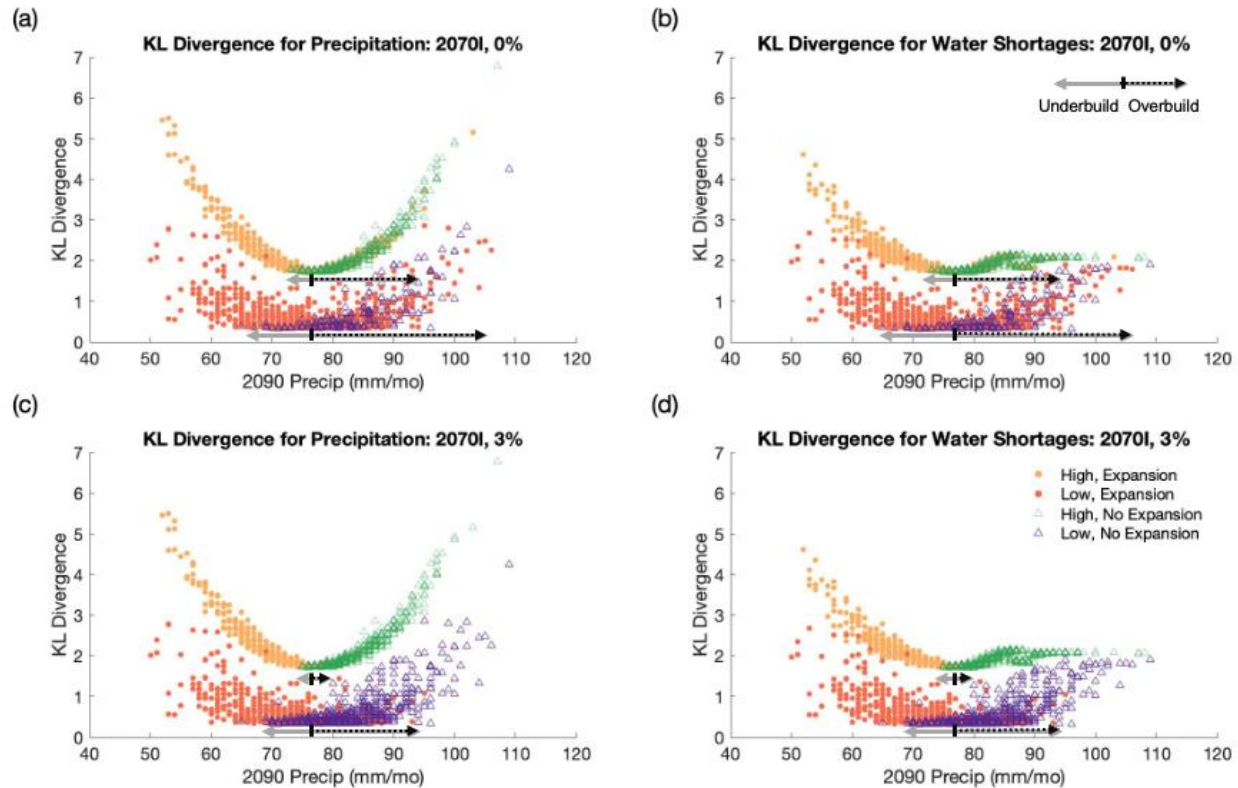
492  
 493 *Figure 7. Static and flexible dam infrastructure and expansion decisions under a) 0% and b) 3% discount rates. The*  
 494 *shaded colors show the frequency that the static dam is chosen (gray) compared to the flexible dam (colors). As the*  
 495 *shading gets darker, the flexible dam expands to a larger volume.*

496 In Figure 7, we illustrate the frequency with which the flexible or static dam is selected,  
 497 and the flexible dam is expanded. In the high-learning climate scenario, the flexible dam is  
 498 selected more frequently, and the least-regret expansion decision is selected more frequently  
 499 compared to the low-learning climate scenario. In panel a under the 0% discount rate, the  
 500 flexible dam is selected 17% and 40% more frequently with high learning than low learning, for  
 501 dry and wet climate simulations, respectively. As conditions progress from dry to wet, the  
 502 flexible dam is chosen more frequently for both high- and low-learning climate scenarios. For  
 503 both discount rates, more overbuilding (dam expansions under wet conditions) and underbuilding  
 504 (less and smaller dam expansions under dry conditions) occurs with low learning, illustrating the  
 505 ability of the optimal policy to choose low-regret actions more effectively in the high-learning  
 506 climate scenario.

507 Finally, we compare KL divergence with dam infrastructure decisions in Figure 8 to  
 508 assess the relationship between the amount of learning about climate uncertainty and flexible  
 509 planning. More learning leads to less over- or underbuilding, and hence, better flexible dam

510 expansion decisions. First, panels a and c show that the relationship between KL divergence for  
 511 precipitation and the 2090 precipitation state has a “U” shape, with more extreme value  
 512 precipitation simulations having higher KL divergence values. Panels b and d show a similar  
 513 relationship between KL divergence for water shortages under dry 2090 precipitation states.  
 514 However, higher KL divergence values for water shortages do not occur in more extreme wet  
 515 precipitation states. As discussed in Figures 3 and 4, above a certain amount of precipitation,  
 516 water shortages do not occur anyway.

517



518  
 519  
 520  
 521  
 522

Figure 8. KL divergence scatter plot for simulations with and without dam expansion under a-b) 0% and c-d) 3% discount rates. The four scatterplots show the correlation between KL divergence for a) and c) precipitation and b) and d) water shortages, compared to the 2090 precipitation state. The different colors and shapes show high and low learning with and without dam expansions from the simulation model.

523  
 524  
 525  
 526  
 527  
 528  
 529  
 530  
 531  
 532

In intermediate precipitation ranges, which we call “transition zones,” samples occur with and without dam expansion. We call policies with unexpanded dams in the left portion of the transition zone “underbuilding,” highlighted with the gray arrows when we have dry 2090 precipitation states, but no dam expansion. We call policies with expanded dams in the right portion of the transition zone “overbuilding,” highlighted with the black arrows when we have wet 2090 precipitation states, but dam expansion. The black vertical lines highlight the initial precipitation state in 1990. With low-learning climate scenarios, transition zones are much larger than with high-learning scenarios. This highlights how more uncertainty in future climate and water availability may lead to less optimal dam infrastructure decisions. The transition zones under low learning are larger on both sides—we have both drier states where the flexible dam

533 does not expand (underbuilding) and wetter states where the flexible dam does expand  
 534 (overbuilding).

535        Additionally, larger transition zones occur with a zero discount rate in panels a and b,  
 536 compared to a 3% discount rate in panels c and d. This is mainly driven by a larger range of  
 537 precipitation states with overbuilding. One hypothesis as to why more overbuilding, but not more  
 538 underbuilding, occurs with zero discounting is because discounting incentivizes delayed  
 539 investment. Therefore, with discounting, the flexible dam is more likely to expand later in the  
 540 planning period because delayed investment is less costly. Without discounting, the flexible dam  
 541 is more likely to be expanded early in the planning period, which could lead to overbuilding.

542 **4 Discussion and Conclusions**

543        In this work, we develop a framework to assess the value of learning in flexible water  
 544 supply infrastructure planning. An exploratory Bayesian modeling approach is used in which we  
 545 adjust the variance of the likelihood function to develop contrasting scenarios where we can  
 546 learn a high or low amount about future climate uncertainty through observation. We assess the  
 547 value of a flexible water supply infrastructure development approach in different climate  
 548 learning scenarios across a range of precipitation conditions. We quantify the value of learning  
 549 for flexibility by first comparing the differences in costs between the static and flexible dams,  
 550 and then comparing those differences across high- and low-learning climates.

551        Our results demonstrate that learning about uncertainty can improve the effectiveness of  
 552 flexible planning in providing low-cost, reliable supply in some but not all conditions. Our  
 553 Bayesian modeling results demonstrate that near-term precipitation observations provide more  
 554 information about long-term precipitation, leading to updated precipitation projections  
 555 substantially narrower than prior estimates. However, these reductions in uncertainty propagate  
 556 non-linearly to water shortage uncertainty, driven by thresholding behavior. Uncertainty in water  
 557 shortage projections is reduced faster than precipitation projections in wetter conditions and  
 558 slower in drier conditions.

559        Similarly, the value of flexibility – and the value of learning for flexibility – is only  
 560 consistently positive in wet precipitation simulations. In these cases, flexibility allows the  
 561 planner to build a smaller dam at the outset of the planning period compared to the static  
 562 development approach and prevents overbuilding of unnecessary new infrastructure. This effect  
 563 is larger in the high-learning climate scenario, where the optimal policy is more consistently able  
 564 to identify the least-regret option. In contrast, with dry climate conditions, flexibility has limited  
 565 value because water reliability is constrained by limited water available to refill the reservoir, not  
 566 limited reservoir storage size. Therefore, regardless of how much learning about future climate  
 567 uncertainty is feasible, there is limited benefit to flexibly expanding dam storage as the climate  
 568 dries because the reservoir is unlikely to refill and utilize additional storage capacity.

569        Since the specific results we highlight depend on the assumptions and context of our case  
 570 study, further sensitivity and uncertainty analysis would help further build theory on the  
 571 conditions under which flexibility is most valuable. Applying this approach to regions with  
 572 different hydroclimate conditions may lead to greater value of learning and flexibility in drying  
 573 conditions. While we focus on long-term precipitation trends, more work can be done assessing

574 impacts of shorter-term uncertainty in precipitation variability, water demands, and dam costs on  
575 total system costs and the value of flexibility. For example, we hypothesize that larger monthly  
576 variability in precipitation or changes in seasonality could increase the value of learning and  
577 flexibility. This is because greater variability would require more storage capacity to maintain  
578 reliable water supply. Therefore, large increases in dam storage would more effectively reduce  
579 shortages compared to our current study. Counterintuitively, it may be that a case study with less  
580 uncertainty in precipitation would see greater value from learning because a single flexible  
581 infrastructure design would be able to adapt more effectively to the full range of possible  
582 outcomes. Additionally, while we focus on uncertainty in long-term precipitation trends, demand  
583 uncertainty due to population growth and economic conditions is likely similarly influential.  
584 Future work could expand the SDP framework to add additional system states for different water  
585 demand conditions and incorporate learning about demand trends.

586 Further work also could assess other forms of both learning and flexibility. This study  
587 focuses on learning by observation. We could also explore learning by model improvement by  
588 comparing precipitation projections from different climate model generations (e.g. CMIP3 vs  
589 CMIP5 vs CMIP6). Similarly, we could explore learning by information collection in a region  
590 with multiple streamflow gauges by holding out then adding additional gauge data. These  
591 approaches may show sharper changes in uncertainty over time rather than the slow gradual  
592 changes here by observation. This could potentially increase the value of learning for flexibility.  
593 Similarly, this study focuses on flexibility in infrastructure design through capacity expansion.  
594 Future work could compare flexibility in planning processes and in operations to compare how  
595 different forms of flexibility interact with different learning scenarios.

596 Our methodological framework to quantify climate learning scenarios and to connect  
597 learning with the value of flexibility can be extended to other infrastructure planning domains.  
598 Climate change uncertainty impacts many planning fields, such as energy (Cohen et al., 2022;  
599 Schaeffer et al., 2012), transportation (Dewar et al., 2008), and natural resources management  
600 (West et al., 2009). Each of these sectors necessitates expensive infrastructure and planning  
601 investments based on uncertain future conditions. Indeed, annual climate change adaptation costs  
602 in lower-income countries are expected to increase from approximately 70 billion USD today to  
603 between 280 and 500 billion USD in 2050 (United Nations Environment Programme, 2021).  
604 Through our methodology to quantify learning about future uncertainty and improve the  
605 usefulness of flexible infrastructure, we improve the theory and approaches that can be used for  
606 adaptive planning. This can support cost-effective climate adaptation, helping target scarce  
607 resources where they are needed most.

## 608 **Acknowledgments**

609 The authors thank three anonymous reviewers for their helpful feedback.

## 610 **Open Research**

611 All data and software used this study can be found at (Skerker, 2023).

## 612 **References**

613 Abramowitz, G., & Bishop, C. H. (2015). Climate Model Dependence and the Ensemble Dependence  
614 Transformation of CMIP Projections. *Journal of Climate*, 28(6), 2332–2348. <https://doi.org/10.1175/JCLI-D-14-00364.1>

615

616 Bellman, R. (1954). Dynamic programming and a new formalism in the calculus of variations. *Proceedings of the  
617 National Academy of Sciences*, 40(4), 231–235. <https://doi.org/10.1073/pnas.40.4.231>

618 Bertoni, F., Giuliani, M., Castelletti, A., & Reed, P. M. (2021). Designing With Information Feedbacks: Forecast  
619 Informed Reservoir Sizing and Operation. *Water Resources Research*, 57(3), e2020WR028112.  
620 <https://doi.org/10.1029/2020WR028112>

621 Brown, C., & Wilby, R. L. (2012). An alternate approach to assessing climate risks. *Eos, Transactions American  
622 Geophysical Union*, 93(41), 401–402. <https://doi.org/10.1029/2012EO410001>

623 Ceres, R. L., Forest, C. E., & Keller, K. (2022). Trade-offs and synergies in managing coastal flood risk: A case  
624 study for New York City. *Journal of Flood Risk Management*, 15(1), e12771.  
625 <https://doi.org/10.1111/jfr3.12771>

626 Cervigni, R., Liden, R., Neumann, J. E., & Strzepek, K. M. (2015). *Enhancing the Climate Resilience of Africa's  
627 Infrastructure: The Power and Water Sectors*. The World Bank. <https://doi.org/10.1596/978-1-4648-0466-3>

628 Cohen, S. M., Dyreson, A., Turner, S., Tidwell, V., Voisin, N., & Miara, A. (2022). A multi-model framework for  
629 assessing long- and short-term climate influences on the electric grid. *Applied Energy*, 317, 119193.  
630 <https://doi.org/10.1016/j.apenergy.2022.119193>

631 Conroy, M. J., Runge, M. C., Nichols, J. D., Stodola, K. W., & Cooper, R. J. (2011). Conservation in the face of  
632 climate change: The roles of alternative models, monitoring, and adaptation in confronting and reducing  
633 uncertainty. *Biological Conservation*, 144(4), 1204–1213. <https://doi.org/10.1016/j.biocon.2010.10.019>

634 Cosgrove, W. J., & Loucks, D. P. (2015). Water management: Current and future challenges and research directions.  
635 *Water Resources Research*, 51(6), 4823–4839. <https://doi.org/10.1002/2014WR016869>

636 Culley, S., Noble, S., Yates, A., Timbs, M., Westra, S., Maier, H. R., Giuliani, M., & Castelletti, A. (2016). A  
637 bottom-up approach to identifying the maximum operational adaptive capacity of water resource systems to  
638 a changing climate. *Water Resources Research*, 52(9), 6751–6768. <https://doi.org/10.1002/2015WR018253>

639 Dewar, J. A., Builder, C. H., Hix, W. M., & Levin, M. H. (1994). *Assumption-based planning: A planning tool for  
640 very uncertain times*. United States Army. <https://apps.dtic.mil/sti/pdfs/ADA282517.pdf>

641 Dewar, J. A., Wachs, M., & RAND Corporation. (2008). *Transportation Planning, Climate Change, and Decision*  
642 *Making under Uncertainty*. <https://rosap.ntl.bts.gov/view/dot/17367>

643 Doss-Gollin, J., & Keller, K. (2022). *A subjective Bayesian framework for synthesizing deep uncertainties in climate*  
644 *risk management* (world). Earth and Space Science Open Archive.  
645 <https://doi.org/10.1002/essoar.10511798.3>

646 Duan, Q., & Phillips, T. J. (2010). Bayesian estimation of local signal and noise in multimodel simulations of  
647 climate change. *Journal of Geophysical Research: Atmospheres*, 115(D18).  
648 <https://doi.org/10.1029/2009JD013654>

649 Ekholm, T. (2018). Climatic Cost-benefit Analysis Under Uncertainty and Learning on Climate Sensitivity and  
650 Damages. *Ecological Economics*, 154, 99–106. <https://doi.org/10.1016/j.ecolecon.2018.07.024>

651 Fletcher, S., Lickley, M., & Strzepek, K. (2019). Learning about climate change uncertainty enables flexible water  
652 infrastructure planning. *Nature Communications*, 10(1), Article 1. [https://doi.org/10.1038/s41467-019-09677-x](https://doi.org/10.1038/s41467-019-<br/>653 09677-x)

654 Fletcher, S., Strzepek, K., Alsaati, A., & Weck, O. de. (2019). Learning and flexibility for water supply  
655 infrastructure planning under groundwater resource uncertainty. *Environmental Research Letters*, 14(11),  
656 114022. <https://doi.org/10.1088/1748-9326/ab4664>

657 Gelman, A., Carlin, J. B., Stern, H. S., Dunson, D. B., Vehtari, A., & Rubin, D. B. (2021). *Bayesian Data Analysis*  
658 (3rd ed.). <http://www.stat.columbia.edu/~gelman/book/BDA3.pdf>

659 Gibson, P. B., Waliser, D. E., Lee, H., Tian, B., & Massoud, E. (2019). Climate Model Evaluation in the Presence of  
660 Observational Uncertainty: Precipitation Indices over the Contiguous United States. *Journal of*  
661 *Hydrometeorology*, 20(7), 1339–1357. <https://doi.org/10.1175/JHM-D-18-0230.1>

662 Giuliani, M., Castelletti, A., Pianosi, F., Mason, E., & Reed, P. M. (2016). Curses, Tradeoffs, and Scalable  
663 Management: Advancing Evolutionary Multiobjective Direct Policy Search to Improve Water Reservoir  
664 Operations. *Journal of Water Resources Planning and Management*, 142(2), 04015050.  
665 [https://doi.org/10.1061/\(ASCE\)WR.1943-5452.0000570](https://doi.org/10.1061/(ASCE)WR.1943-5452.0000570)

666 Giuliani, M., Zaniolo, M., Castelletti, A., Davoli, G., & Block, P. (2019). Detecting the State of the Climate System  
667 via Artificial Intelligence to Improve Seasonal Forecasts and Inform Reservoir Operations. *Water*  
668 *Resources Research*, 55(11), 9133–9147. <https://doi.org/10.1029/2019WR025035>

669 Gleick, P. H. (1989). Climate change, hydrology, and water resources. *Reviews of Geophysics*, 27(3), 329–344.  
670 <https://doi.org/10.1029/RG027i003p00329>

671 Gleick, P. H. (2000). *Water: The Potential Consequences of Climate Variability and Change for the Water*  
672 *Resources of the United States*. Pacific Institute for Studies in Development, Environment, and Security.  
673 <https://d3pcsg2wjq9izr.cloudfront.net/files/6846/articles/4084/4084.pdf>

674 Gong, W., Yang, D., Gupta, H. V., & Nearing, G. (2014). Estimating information entropy for hydrological data:  
675 One-dimensional case. *Water Resources Research*, 50(6), 5003–5018.  
676 <https://doi.org/10.1002/2014WR015874>

677 Haasnoot, M., Kwakkel, J. H., Walker, W. E., & ter Maat, J. (2013). Dynamic adaptive policy pathways: A method  
678 for crafting robust decisions for a deeply uncertain world. *Global Environmental Change*, 23(2), 485–498.  
679 <https://doi.org/10.1016/j.gloenvcha.2012.12.006>

680 Herman, J. D., Quinn, J. D., Steinschneider, S., Giuliani, M., & Fletcher, S. (2020). Climate Adaptation as a Control  
681 Problem: Review and Perspectives on Dynamic Water Resources Planning Under Uncertainty. *Water*  
682 *Resources Research*, 56(2), e24389. <https://doi.org/10.1029/2019WR025502>

683 Hui, R., Herman, J., Lund, J., & Madani, K. (2018). Adaptive water infrastructure planning for nonstationary  
684 hydrology. *Advances in Water Resources*, 118, 83–94. <https://doi.org/10.1016/j.advwatres.2018.05.009>

685 IPCC. (2022). *Climate Change 2022: Impacts, Adaptation and Vulnerability*. Contribution of Working Group II to  
686 the Sixth Assessment Report of the Intergovernmental Panel on Climate Change [H.-O. Pörtner, D.C.  
687 Roberts, M. Tignor, E.S. Poloczanska, K. Mintenbeck, A. Alegría, M. Craig, S. Langsdorf, S. Löschke, V.  
688 Möller, A. Okem, B. Rama (eds.)].

689 Kermisch, C., & Taebi, B. (2017). Sustainability, Ethics and Nuclear Energy: Escaping the Dichotomy.  
690 *Sustainability*, 9(3), Article 3. <https://doi.org/10.3390/su9030446>

691 Kullback, S., & Leibler, R. A. (1951). On Information and Sufficiency. *The Annals of Mathematical Statistics*,  
692 22(1), 79–86.

693 Kumar, S., Merwade, V., Kinter, J. L., & Niyogi, D. (2013). Evaluation of Temperature and Precipitation Trends  
694 and Long-Term Persistence in CMIP5 Twentieth-Century Climate Simulations. *Journal of Climate*, 26(12),  
695 4168–4185. <https://doi.org/10.1175/JCLI-D-12-00259.1>

696 Kwakkel, J. H., Haasnoot, M., & Walker, W. E. (2015). Developing dynamic adaptive policy pathways: A  
697 computer-assisted approach for developing adaptive strategies for a deeply uncertain world. *Climatic  
698 Change*, 132(3), 373–386. <https://doi.org/10.1007/s10584-014-1210-4>

699 Kwakkel, J. H., Haasnoot, M., & Walker, W. E. (2016). Comparing Robust Decision-Making and Dynamic  
700 Adaptive Policy Pathways for model-based decision support under deep uncertainty. *Environmental  
701 Modelling & Software*, 86, 168–183. <https://doi.org/10.1016/j.envsoft.2016.09.017>

702 Lamontagne, J. R., Reed, P. M., Link, R., Calvin, K. V., Clarke, L. E., & Edmonds, J. A. (2018). Large Ensemble  
703 Analytic Framework for Consequence-Driven Discovery of Climate Change Scenarios. *Earth's Future*,  
704 6(3), 488–504. <https://doi.org/10.1002/2017EF000701>

705 Leung, L.-Y., & North, G. R. (1990). Information Theory and Climate Prediction. *Journal of Climate*, 3(1), 5–14.  
706 [https://doi.org/10.1175/1520-0442\(1990\)003<0005:ITACP>2.0.CO;2](https://doi.org/10.1175/1520-0442(1990)003<0005:ITACP>2.0.CO;2)

707 Marescot, L., Chapron, G., Chadès, I., Fackler, P. L., Duchamp, C., Marboutin, E., & Gimenez, O. (2013). Complex  
708 decisions made simple: A primer on stochastic dynamic programming. *Methods in Ecology and Evolution*,  
709 4(9), 872–884. <https://doi.org/10.1111/2041-210X.12082>

710 Marin, J.-M., & Robert, C. P. (2007). *Bayesian Core: A Practical Approach to Computational Bayesian Statistics*.  
711 Springer. <https://doi.org/10.1007/978-0-387-38983-7>

712 Massoud, E. C., Lee, H., Gibson, P. B., Loikith, P., & Waliser, D. E. (2020). Bayesian Model Averaging of Climate  
713 Model Projections Constrained by Precipitation Observations over the Contiguous United States. *Journal of  
714 Hydrometeorology*, 21(10), 2401–2418. <https://doi.org/10.1175/JHM-D-19-0258.1>

715 Moore, A. L., & McCarthy, M. A. (2010). On Valuing Information in Adaptive-Management Models. *Conservation  
716 Biology*, 24(4), 984–993. <https://doi.org/10.1111/j.1523-1739.2009.01443.x>

717 Mortazavi-Naeini, M., Kuczera, G., Kiem, A. S., Cui, L., Henley, B., Berghout, B., & Turner, E. (2015). Robust  
718 optimization to secure urban bulk water supply against extreme drought and uncertain climate change.  
719 *Environmental Modelling & Software*, 69, 437–451. <https://doi.org/10.1016/j.envsoft.2015.02.021>

720 Nearing, G. S., & Gupta, H. V. (2015). The quantity and quality of information in hydrologic models. *Water  
721 Resources Research*, 51(1), 524–538. <https://doi.org/10.1002/2014WR015895>

722 Ojwang, R. O., Dietrich, J., Anebagilu, P. K., Beyer, M., & Rottensteiner, F. (2017). Rooftop Rainwater Harvesting  
723 for Mombasa: Scenario Development with Image Classification and Water Resources Simulation. *Water*,  
724 9(5), Article 5. <https://doi.org/10.3390/w9050359>

725 Pahl-Wostl, C. (2007). Transitions towards adaptive management of water facing climate and global change. *Water  
726 Resources Management*, 21(1), 49–62. <https://doi.org/10.1007/s11269-006-9040-4>

727 Paton, F. L., Maier, H. R., & Dandy, G. C. (2014). Including adaptation and mitigation responses to climate change  
728 in a multiobjective evolutionary algorithm framework for urban water supply systems incorporating GHG  
729 emissions. *Water Resources Research*, 50(8), 6285–6304. <https://doi.org/10.1002/2013WR015195>

730 Pulwarty, R. S., & Melis, T. S. (2001). Climate extremes and adaptive management on the Colorado River: Lessons  
731 from the 1997–1998 ENSO event. *Journal of Environmental Management*, 63(3), 307–324.  
732 <https://doi.org/10.1006/jema.2001.0494>

733 Quinn, J. D., Hadjimichael, A., Reed, P. M., & Steinschneider, S. (2020). Can Exploratory Modeling of Water  
734 Scarcity Vulnerabilities and Robustness Be Scenario Neutral? *Earth's Future*, 8(11), e2020EF001650.  
735 <https://doi.org/10.1029/2020EF001650>

736 Raso, L., Barbier, B., & Bader, J.-C. (2019). Modeling dynamics and adaptation at operational and structural scales  
737 for the ex-ante economic evaluation of large dams in an African context. *Water Resources and Economics*,  
738 26. Scopus. <https://doi.org/10.1016/j.wre.2018.08.001>

739 Ruosteenoja, K., Tuomenvirta, H., & Jylhä, K. (2007). GCM-based regional temperature and precipitation change  
740 estimates for Europe under four SRES scenarios applying a super-ensemble pattern-scaling method.  
741 *Climatic Change*, 81(S1), 193–208. <https://doi.org/10.1007/s10584-006-9222-3>

742 Sanderson, B. M., Wehner, M., & Knutti, R. (2017). Skill and independence weighting for multi-model assessments.  
743 *Geoscientific Model Development*, 10(6), 2379–2395. <https://doi.org/10.5194/gmd-10-2379-2017>

744 Schaeffer, R., Szklo, A. S., Pereira de Lucena, A. F., Moreira Cesar Borba, B. S., Pupo Nogueira, L. P., Fleming, F.  
745 P., Troccoli, A., Harrison, M., & Boulahya, M. S. (2012). Energy sector vulnerability to climate change: A  
746 review. *Energy*, 38(1), 1–12. <https://doi.org/10.1016/j.energy.2011.11.056>

747 Skerker, J. (2023). *jskerker/QuantLearning: Data and Code for Quantifying the Value of Learning for Flexible  
748 Water Infrastructure Planning* (v1.0) [Zenodo]. <https://doi.org/10.5281/zenodo.7844018>

749 Smith, R. L., Tebaldi, C., Nychka, D., & Mearns, L. O. (2009). Bayesian Modeling of Uncertainty in Ensembles of  
750 Climate Models. *Journal of the American Statistical Association*, 104(485), 97–116.  
751 <https://doi.org/10.1198/jasa.2009.0007>

752 Spiller, M., Vreeburg, J. H. G., Leusbroek, I., & Zeeman, G. (2015). Flexible design in water and wastewater  
753 engineering – Definitions, literature and decision guide. *Journal of Environmental Management*, 149, 271–  
754 281. <https://doi.org/10.1016/j.jenvman.2014.09.031>

755 Stakhiv, E. Z. (2011). Pragmatic Approaches for Water Management Under Climate Change Uncertainty. *JAWRA*  
756 *Journal of the American Water Resources Association*, 47(6), 1183–1196. <https://doi.org/10.1111/j.1752-1688.2011.00589.x>

758 State Department of Natural Water Services. (2016). *Water Security and Climate Resilience in the Coastal Region, Kenya: Environmental and Social Impact Assessment Study Report*.

759

760 Steinschneider, S., McCrary, R., Mearns, L. O., & Brown, C. (2015). The effects of climate model similarity on  
761 probabilistic climate projections and the implications for local, risk-based adaptation planning. *Geophysical  
762 Research Letters*, 42(12), 5014–5044. <https://doi.org/10.1002/2015GL064529>

763 Storck, P., Eheart, J. W., & Valocchi, A. J. (1997). A method for the optimal location of monitoring wells for  
764 detection of groundwater contamination in three-dimensional heterogenous aquifers. *Water Resources  
765 Research*, 33(9), 2081–2088. <https://doi.org/10.1029/97WR01704>

766 Tebaldi, C. (2004). Regional probabilities of precipitation change: A Bayesian analysis of multimodel simulations.  
767 *Geophysical Research Letters*, 31(24), L24213. <https://doi.org/10.1029/2004GL021276>

768 Tebaldi, C., & Knutti, R. (2007). The use of the multi-model ensemble in probabilistic climate projections.  
769 *Philosophical Transactions of the Royal Society A: Mathematical, Physical and Engineering Sciences*,  
770 365(1857), 2053–2075. <https://doi.org/10.1098/rsta.2007.2076>

771 Tebaldi, C., Smith, R. L., Nychka, D., & Mearns, L. O. (2005). Quantifying Uncertainty in Projections of Regional  
772 Climate Change: A Bayesian Approach to the Analysis of Multimodel Ensembles. *Journal of Climate*,  
773 18(10), 1524–1540. <https://doi.org/10.1175/JCLI3363.1>

774 United Nations Environment Programme. (2021). *Adaptation Gap Report 2020*.  
775 <http://www.unep.org/resources/adaptation-gap-report-2020>

776 Urban, N. M., Holden, P. B., Edwards, N. R., Srivat, R. L., & Keller, K. (2014). Historical and future learning about  
777 climate sensitivity. *Geophysical Research Letters*, 41(7), 2543–2552.  
778 <https://doi.org/10.1002/2014GL059484>

779 Urban, N. M., & Keller, K. (2010). Probabilistic hindcasts and projections of the coupled climate, carbon cycle and  
780 Atlantic meridional overturning circulation system: A Bayesian fusion of century-scale observations with a  
781 simple model. *Tellus A: Dynamic Meteorology and Oceanography*, 62(5), 737–750.  
782 <https://doi.org/10.1111/j.1600-0870.2010.00471.x>

783 Walker, W. E., Rahman, S. A., & Cave, J. (2001). Adaptive policies, policy analysis, and policymaking. *European  
784 Journal of Operation Research*.  
785 [https://www.sciencedirect.com/science/article/pii/S0377221700000710?casa\\_token=DcRzbE2y8UAAAAA  
AA:VfYJ21zgKMW0oZRw\\_jXJj\\_88rRv0wNTIPxqISfL85f\\_nfCAqR9ECX31R-STRBTRtfGi-FNmyhA](https://www.sciencedirect.com/science/article/pii/S0377221700000710?casa_token=DcRzbE2y8UAAAAA<br/>786 AA:VfYJ21zgKMW0oZRw_jXJj_88rRv0wNTIPxqISfL85f_nfCAqR9ECX31R-STRBTRtfGi-FNmyhA)

787 Walters, C. (1997). Challenges in adaptive management of riparian and coastal ecosystems. *Conservation Ecology*,  
788 1(2). <https://www.jstor.org/stable/26271661>

789 Weijs, S. V., Schoups, G., & van de Giesen, N. (2010). Why hydrological predictions should be evaluated using  
790 information theory. *Hydrology and Earth System Sciences*, 14(12), 2545–2558.  
791 <https://doi.org/10.5194/hess-14-2545-2010>

792 West, J. M., Julius, S. H., Kareiva, P., Enquist, C., Lawler, J. J., Petersen, B., Johnson, A. E., & Shaw, M. R. (2009).  
793 U.S. Natural Resources and Climate Change: Concepts and Approaches for Management Adaptation.  
794 *Environmental Management*, 44(6), 1001. <https://doi.org/10.1007/s00267-009-9345-1>

795 Williams, B. K. (2011). Adaptive management of natural resources—Framework and issues. *Journal of  
796 Environmental Management*, 92(5), 1346–1353. <https://doi.org/10.1016/j.jenvman.2010.10.041>

797 Williams, B. K., & Brown, E. D. (2016). Technical challenges in the application of adaptive management.  
798 *Biological Conservation*, 195, 255–263. <https://doi.org/10.1016/j.biocon.2016.01.012>

799 Woodward, M., Kapelan, Z., & Gouldby, B. (2014). Adaptive Flood Risk Management Under Climate Change  
800 Uncertainty Using Real Options and Optimization. *Risk Analysis*, 34(1), 75–92.  
801 <https://doi.org/10.1111/risa.12088>

802 Zaniolo, M., Giuliani, M., & Castelletti, A. (2021). Policy Representation Learning for Multiobjective Reservoir  
803 Policy Design With Different Objective Dynamics. *Water Resources Research*, 57(12), e2020WR029329.  
804 <https://doi.org/10.1029/2020WR029329>

805 Zeff, H., Herman, J. D., Reed, P. M., & Characklis, G. W. (2016). Cooperative drought adaptation: Integrating  
806 infrastructure development, conservation, and water transfers into adaptive policy pathways. *Water  
807 Resources Research*, 52(9), 7327–7346. <https://doi.org/10.1002/2016WR018771>

808

809 **Supporting Information References**